

each other. Altogether, by use of these organic-inorganic building blocks, a specific and rational crystalline arrangement is achieved. We believe that this could be the base for further substitution at particular molecular ion sites in order to modify such unique properties of this hybrid salt as the peculiar slight expansion of the metal-metal bond lengths in the Nb₆ cluster core or the organic dimer-metal cluster magnetic interaction.

Acknowledgment. We thank the C.N.R.S. (ATP-PIRMAT Chimie Douce) for their support, Dr. L. Ducasse

of Université de Bordeaux I for the intradimer transfer integral calculation, and Dr. P. Guénot, Université de Rennes I, for the mass spectrometry experiments.

Registry No. TTF, 31366-25-3; (TTF)₂(Nb₆Cl₁₈)(Et₄N)-(CH₃CN), 124854-80-4; (Et₄N)₃Nb₆Cl₁₈, 12128-45-9.

Supplementary Material Available: Tables of atomic coordinates (including hydrogen atoms), anisotropic thermal parameters, and all bond lengths and angles (4 pages); observed and calculated structure factors (5 pages). Ordering information is given on any current masthead page.

Novel Redox Properties of the Paramagnetic Hexanuclear Niobium Cluster Halide Nb₆Cl₁₈³⁻ and the Preparation, Structures, and Conducting and Magnetic Properties of Its One-Dimensional Mixed-Valence Tetramethyltetra(selena and thia)fulvalenium Salts: [TMTSF and TMTTF]₅[Nb₆Cl₁₈]·(CH₂Cl₂)_{0.5}

Alain Pénicaud and Patrick Batail*

*Laboratoire de Physique des Solides Associé au CNRS, Université de Paris-Sud,
91405 Orsay, France*

Claude Coulon

*Centre de Recherche Paul Pascal, CNRS, Domaine Universitaire de Bordeaux I,
33405 Talence, France*

Enric Canadell

*Laboratoire de Chimie Théorique Associé au CNRS, Université de Paris-Sud,
91405 Orsay, France*

Christiane Perrin

*Laboratoire de Chimie Minérale B Associé au CNRS, Université de Rennes I,
35042 Rennes, France*

Received July 31, 1989

A cyclic voltammetry study in acetonitrile of [(C₂H₅)₄N]₃Nb₆Cl₁₈ is presented that gives the first evidence for the existence at 1.72 V vs SCE of the 13-electron cluster core Nb₆Cl₁₂⁵⁺, a novel powerful inorganic oxidant. The title compounds have been prepared by electrocrystallization and characterized by single-crystal X-ray diffraction, ESR, and magnetic susceptibility and transport experiments. [(D)₄³⁺(D⁰)]Nb₆Cl₁₈³⁻(CH₂Cl₂)_{0.5} [D = 2,3,6,7-tetramethyl-1,4,5,8-selena- and thiafulvalene (TMTSF and TMTTF) in 1 and 2, respectively] are semiconducting ($\sigma_{300\text{K}} = 0.5 \Omega^{-1} \text{cm}^{-1}$ for 1; activation energies of 0.16 and 0.20 eV for 1 and 2, respectively) and the triclinic (space group *P* $\bar{1}$) unit-cell parameters are $a = 13.176$ (5), $b = 13.847$ (7), $c = 14.581$ (9) Å, $\alpha = 113.79$ (3), $\beta = 96.47$ (3), $\gamma = 99.94$ (3)°, $V = 2348.1$ (2) Å³ for 1 and $a = 12.933$ (7), $b = 13.669$ (8), $c = 14.334$ (11) Å, $\alpha = 114.40$ (3), $\beta = 96.97$ (4), $\gamma = 99.21$ (4)°, $V = 2227.8$ (3) Å³ for 2. Both salts are isostructural and present stacks of the organic radical cations with one-dimensional electronic properties. The electronic structure of these salts has been studied by means of tight-binding band structure calculations. A unique magnetic interaction between the organic spins and the localized inorganic cluster spins is presented and discussed.

Introduction

Since the pioneering work of Siedle,¹ the chemistry of tetrathiafulvalene (TTF) and its substituted derivatives with transition-metal halides has been expanding rapidly

with the aim of combining highly anisotropic electrical properties and extended TTF-metal interactions. Many different types of materials have been prepared based on discrete and polymeric inorganic metal halides with a variety of coordination geometries.² In addition, oxidizing organometallic halides have recently been engaged in

(1) (a) Siedle, A. R.; Candela, G. A.; Finnegan, T. F.; Van Duyne, R. P.; Cape, T.; Kokoszka, G. F.; Woyciesjes, P. M.; Hashmall, J. A.; Glick, M.; Isley, W. *Ann. N.Y. Acad. Sci.* **1978**, *313*, 377. (b) Siedle, A. R. *Extended Linear Chain Compounds*; Miller, J. S., Ed.; Plenum Press: New York, 1982; p 469.

(2) For a recent survey, see the proceedings of the International Conference on Science and Technology of Synthetic Metals, Santa Fe; *Synth. Met.* **1988**, *27*, nos. 1-4.

TTF-based charge-transfer salts.³ As noted earlier, inorganic cluster compounds are "sophisticated redox systems in the solid state, and simultaneously potential generators of interesting molecular compounds".⁴ We recently developed⁵ a series of TTF-based hybrid salts of the isostructural and isoelectronic all-inorganic hexanuclear molecular cluster halides and chalcogenides $\text{Mo}_6\text{Cl}_8(\text{Cl}_6)^{2-}$ (ref 5a) and $\text{Re}_6\text{Se}_5\text{Cl}_3(\text{Cl}_6)^-$ (ref 5b) designed to exploit some of their specific features such as their size, shape, charge, and HOMO-LUMO gap in the construction of new molecular solids. In particular, it was found that changing the charge of the anion resulted in profound modifications of the structural and electronic properties of the salts. In this paper we present the first electrochemical evidence for the existence of the 13-electron cluster anion $\text{Nb}_6\text{Cl}_{12}(\text{Cl}_6)^-$, a novel powerful inorganic oxidant. We then report⁶ on the preparation, crystal and band electronic structures, and conducting and magnetic properties of the tetramethyltetra(seleena and thia)fulvalenium salts of the trivalent and paramagnetic hexanuclear niobium cluster halide $\text{Nb}_6\text{Cl}_{12}(\text{Cl}_6)^{3-}$ and demonstrate that in spite of the large size and charge of the cluster anion, stacks of radical cations with one-dimensional electronic properties are stabilized in these compounds. The one-dimensional character of these salts is not preserved when combining the same cluster anion with TTF, a very similar donor only slightly different in size and shape. Rather, discrete organic dimers are stabilized in a unique tridimensional structure described in the accompanying contribution.⁷

Experimental Section

Preparation of $(\text{TMTSF})_5(\text{Nb}_6\text{Cl}_{18}) \cdot (\text{CH}_2\text{Cl}_2)_{0.5}$ (1) and $(\text{TMTTF})_5(\text{Nb}_6\text{Cl}_{18}) \cdot (\text{CH}_2\text{Cl}_2)_{0.5}$ (2). The solvents were dried and degassed prior to utilization, and the electrochemical cells degassed with argon. Black, shiny, needlelike single crystals of 1 and 2 were grown at a platinum wire anode under constant-current electrolysis ($J = 1.8 \mu\text{A cm}^{-2}$, 19 days) of 25 cm³ of a $\text{CH}_3\text{CN}:\text{CH}_2\text{Cl}_2$ (4:1) solution (passed over activated neutral alumina) containing the donor (TMTSF,⁸ 22 mg, 0.05 mmol, or TMTTF,⁹ 13 mg, 0.05 mmol, both recrystallized three times and sublimated) and $(\text{Et}_4\text{N})_3\text{Nb}_6\text{Cl}_{18}$ (0.12 g, 0.076 mmol). The latter was prepared as described previously.¹⁰ The composition and amount of solvent of crystallization were determined by resolution of the crystal structure.

Electrochemical Measurements. Cyclic voltammograms were recorded by using a PAR 273 potentiostat with Pt and vitreous carbon working and auxiliary electrodes respectively, a SCE reference electrode, and $\text{Bu}_4\text{N}^+\text{PF}_6^-$ as supporting elec-

Table I. Atomic Coordinates ($\times 10^4$) and Equivalent Isotropic Thermal Parameter for 1, Excluding Hydrogen and Solvent Atoms

atom	x	y	z	$B_{\text{eq}}/\text{\AA}^2$
Nb(1)	299.9 (9)	968.5 (8)	-803.3 (9)	1.86 (2)
Nb(2)	-1601.6 (9)	-531.9 (9)	-754.5 (9)	1.90 (3)
Nb(3)	-346.8 (9)	1324.5 (9)	1189.8 (9)	1.92 (3)
Cl(1)	749 (3)	-413 (3)	-2280 (3)	2.79 (8)
Cl(2)	-1480 (3)	475 (3)	-1799 (3)	2.64 (7)
Cl(3)	-2239 (3)	886 (3)	515 (3)	2.73 (8)
Cl(4)	2172 (3)	1732 (3)	-38 (3)	2.60 (7)
Cl(5)	-56 (3)	2626 (2)	447 (3)	2.54 (7)
Cl(6)	-1436 (3)	-2119 (3)	-2234 (3)	2.72 (8)
Cl(7)	631 (3)	2137 (3)	-1759 (3)	3.22 (8)
Cl(8)	-3509 (3)	-1141 (3)	-1651 (3)	3.67 (9)
Cl(9)	-746 (3)	2927 (3)	2606 (3)	3.64 (9)
Se(1)	6800 (1)	5706 (1)	311 (1)	2.62 (3)
Se(2)	5365 (1)	3309 (1)	-754 (1)	2.73 (3)
C(1)	5440 (10)	4790 (10)	-100 (10)	2.3 (3)
C(2)	7410 (10)	4510 (10)	-130 (10)	3.0 (3)
C(3)	6850 (10)	3530 (10)	-580 (10)	2.3 (3)
C(4)	8630 (10)	4820 (10)	40 (10)	3.4 (4)
C(5)	7220 (10)	2500 (10)	-960 (10)	4.2 (4)
Se(3)	4064 (1)	3953 (1)	7022 (1)	2.80 (3)
Se(4)	5602 (1)	6282 (1)	8005 (1)	2.90 (3)
Se(5)	7680 (1)	5198 (1)	7675 (1)	2.84 (3)
Se(6)	6211 (1)	2836 (1)	6664 (1)	2.62 (3)
C(6)	5440 (10)	4780 (10)	7410 (10)	2.3 (3)
C(7)	6310 (10)	4320 (10)	7270 (10)	2.6 (3)
C(8)	3500 (10)	5180 (10)	7500 (10)	2.9 (3)
C(9)	4140 (10)	6150 (10)	7920 (10)	2.8 (3)
C(10)	8290 (10)	3990 (10)	7230 (10)	3.3 (4)
C(11)	7660 (10)	3000 (10)	6810 (10)	2.8 (3)
C(12)	2300 (10)	4900 (10)	7350 (10)	4.5 (5)
C(13)	3870 (10)	7240 (10)	8350 (10)	4.3 (4)
C(14)	9480 (10)	4280 (10)	7420 (10)	3.7 (4)
C(15)	8040 (10)	1940 (10)	6440 (10)	3.7 (4)
Se(7)	5365 (1)	3297 (1)	4332 (1)	3.57 (4)
Se(8)	6803 (1)	5672 (1)	5396 (1)	3.83 (4)
C(16)	5430 (10)	4770 (10)	4936 (9)	2.6 (3)
C(17)	6860 (10)	3530 (10)	4460 (10)	3.5 (4)
C(18)	7410 (10)	4470 (10)	4870 (10)	4.1 (5)
C(19)	7200 (10)	2400 (10)	4040 (10)	5.4 (6)
C(20)	8640 (10)	4820 (10)	5120 (10)	4.8 (5)
Se(9)	3689 (1)	820 (1)	5667 (1)	3.53 (4)
Se(10)	5342 (1)	-202 (1)	6523 (1)	3.54 (4)
C(21)	4820 (10)	100 (10)	5420 (10)	4.1 (4)
C(22)	3700 (10)	830 (10)	6980 (10)	2.9 (3)
C(23)	4370 (10)	390 (10)	7330 (10)	3.9 (4)
C(24)	2860 (10)	1350 (10)	7480 (10)	3.8 (4)
C(25)	4400 (10)	300 (10)	8330 (10)	4.2 (4)

trolyte in acetonitrile. A ferrocene internal standard ($\text{Fc}^{+/0}$ couple) was measured after each experiment at 0.39 V vs the SCE reference.

Crystal Data. 1: $\text{C}_{50}\text{H}_{60}\text{Cl}_{18}\text{Nb}_6\text{Se}_{20}(\text{CH}_2\text{Cl}_2)_{0.5}$, FW = 3478.29; triclinic, $a = 13.176$ (5), $b = 13.847$ (7), $c = 14.581$ (9) \AA , $\alpha = 113.79$ (3), $\beta = 96.47$ (3), $\gamma = 99.94$ (3)°, $V = 2348.1$ (2) \AA^3 (determined by least-squares refinement of the angular coordinates of 25 accurately centered reflections with θ varying from 11 to 20°); Mo K α radiation, $\lambda = 0.71069$ \AA ; space group $P\bar{1}$, $Z = 1$, $D_x = 2.46$ g cm⁻³; crystal dimensions $0.21 \times 0.19 \times 0.04$ mm³, $\mu = 89$ cm⁻¹. 2: $\text{C}_{50}\text{H}_{60}\text{Cl}_{18}\text{Nb}_6\text{S}_{20}(\text{CH}_2\text{Cl}_2)_{0.5}$, FW = 2540.37; triclinic, $a = 12.933$ (7), $b = 13.669$ (8), $c = 14.334$ (11) \AA , $\alpha = 114.40$ (3), $\beta = 96.97$ (4), $\gamma = 99.21$ (4)°, $V = 2227.8$ (3) \AA^3 (determined by least-squares refinement of the angular coordinates of 22 reflections with θ varying from 11 to 18°); Mo K α radiation, $\lambda = 0.71069$ \AA ; space group $P\bar{1}$, $Z = 1$, $D_x = 1.89$ g cm⁻³; crystal dimensions $0.20 \times 0.17 \times 0.03$ mm³, $\mu = 17$ cm⁻¹.

Data Collection and Processing.¹¹ An Enraf-Nonius CAD4-F diffractometer, $\omega/2\theta$ mode with ω scan width $1 + 0.35 \tan \theta$, and graphite-monochromated Mo K α radiation were used. 1: 8562 reflections measured ($1 \leq \theta \leq 26^\circ$, $-h, +h, -k, +k, 0, l$), 8206 unique reflections (merging $R = 1.2\%$) of which 5154 re-

(3) Morse, D. B.; Rauchfuss, T. B.; Wilson, S. R. *J. Am. Chem. Soc.* **1988**, *110*, 2646.

(4) von Schnering, H. G. *Angew. Chem. Intl. Ed. Engl.* **1981**, *20*, 33; see also: Hughbanks, T.; Hoffmann, R. *J. Am. Chem. Soc.* **1983**, *105*, 1150.

(5) (a) Batail, P.; Ouahab, L. *Mol. Cryst. Liq. Cryst.* **1985**, *125*, 205; Ouahab, L.; Batail, P.; Perrin, C.; Garrigou-Lagrange, C. *Mat. Res. Bull.* **1986**, *21*, 1223; (b) Batail, P.; Ouahab, L.; Penicaud, A.; Lenoir, C.; Perrin, A. C. R. *Hebd. Seances Acad. Sc.* **1987**, *304* sér. II, 1111; Renault A.; Pouget, J. P.; Parkin, S.S.P.; Torrance, J. B.; Ouahab, L.; Batail, P. *Mol. Cryst. Liq. Cryst.* **1988**, *161*, 329; Penicaud, A.; Lenoir, C.; Batail, P.; Coulon, C.; Perrin, A. *Synth. Metals.*, **1989**, *32*, 25; Penicaud, A.; Boubekeur, K.; Batail, P.; Coulon, C.; Perrin, A.; Auban, P.; Jérôme, D. to be submitted.

(6) (a) A preliminary report of this work has been published: Penicaud, A.; Batail, P.; Perrin, C.; Coulon, C.; Parkin, S. S. P.; Torrance, J. B. *J. Chem. Soc., Chem. Commun.* **1987**, 330.

(7) Penicaud, A.; Batail, P.; Davidson, P.; Levelut, A.-M.; Coulon, C.; Perrin, C. *Chem. Mater.*, preceding paper in this issue.

(8) Bechgaard, K.; Cowan, D. O.; Bloch, A. N. *J. Chem. Soc., Chem. Commun.* **1974**, 937.

(9) Wudl, F. *Chemistry and physics of 1D metals*; Keller, H. J., Ed.; Plenum Press: New York, 1977; Vol. B25, 233.

(10) (a) Koknat, F. W.; Parson, J. A.; Gongvusharina, A. *Inorg. Chem.* **1974**, *13*, 7. (b) Mackay, R. A.; Schneider, R. F. *Inorg. Chem.* **1967**, *6*, 549.

(11) Frenz, B. A. *Computing in Crystallography*; Delft University Press: Delft, The Netherlands, 1978.

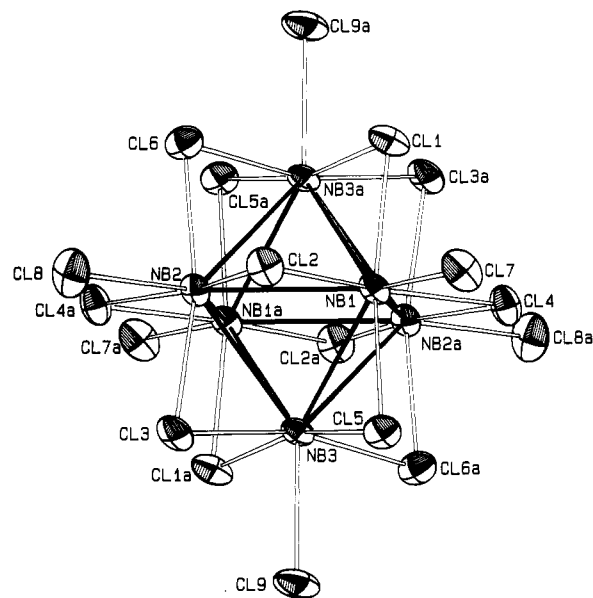
Table II. Atomic Coordinates ($\times 10^4$) and Equivalent Isotropic Thermal Parameter for 2, Excluding Hydrogen and Solvent Atoms

atom	x	y	z	$B_{eq}/\text{\AA}^2$
Nb(1)	260.9 (7)	935.1 (6)	-851.3 (7)	2.11 (2)
Nb(2)	-1628.0 (7)	-600.1 (6)	-788.7 (7)	2.15 (2)
Nb(3)	-394.5 (7)	1350.6 (6)	1180.1 (7)	2.14 (2)
Cl(1)	769 (2)	-478 (2)	-2320 (2)	2.89 (7)
Cl(2)	-1560 (2)	372 (2)	-1881 (2)	2.87 (7)
Cl(3)	-2324 (2)	844 (2)	465 (2)	2.90 (7)
Cl(4)	2160 (2)	1776 (2)	-59 (2)	2.91 (7)
Cl(5)	-143 (2)	2626 (2)	392 (2)	2.76 (7)
Cl(6)	-1405 (2)	-2228 (2)	-2261 (2)	2.99 (7)
Cl(7)	534 (2)	2057 (2)	-1872 (2)	3.43 (7)
Cl(8)	-3558 (2)	-1291 (2)	-1731 (2)	3.78 (8)
Cl(9)	-855 (2)	2991 (2)	2579 (2)	3.66 (8)
S(1)	6724 (2)	5650 (2)	267 (2)	3.17 (8)
S(2)	5382 (2)	3392 (2)	-758 (2)	3.23 (8)
C(1)	5450 (8)	4805 (7)	-96 (8)	2.6 (3)
C(2)	7383 (8)	4566 (7)	-176 (8)	2.9 (3)
C(3)	6781 (8)	3541 (8)	-633 (8)	3.1 (3)
C(4)	8583 (9)	4908 (9)	23 (9)	4.0 (3)
C(5)	7136 (9)	2482 (8)	-1046 (9)	3.6 (3)
S(3)	4129 (2)	3970 (2)	7015 (2)	3.31 (8)
S(4)	5549 (2)	6155 (2)	7979 (2)	3.33 (8)
S(5)	7587 (2)	5100 (2)	7612 (2)	3.21 (8)
S(6)	6209 (2)	2891 (2)	6620 (2)	3.14 (8)
C(6)	5429 (8)	4748 (7)	7376 (8)	2.7 (3)
C(7)	6310 (8)	4304 (7)	7233 (8)	2.7 (3)
C(8)	3508 (8)	5084 (7)	7488 (8)	3.0 (3)
C(9)	4171 (8)	6100 (8)	7938 (9)	3.4 (3)
C(10)	8225 (7)	4025 (7)	7207 (8)	2.6 (3)
C(11)	7590 (8)	2997 (7)	6752 (8)	3.2 (3)
C(12)	2324 (9)	4790 (9)	7370 (10)	4.4 (3)
C(13)	3879 (9)	7171 (8)	8406 (9)	4.2 (3)
C(14)	9429 (9)	4304 (9)	7420 (10)	4.7 (4)
C(15)	7941 (9)	1922 (8)	6355 (9)	4.1 (3)
S(7)	5412 (3)	3403 (3)	4331 (3)	5.8 (1)
S(8)	6723 (3)	5632 (3)	5363 (3)	5.7 (1)
C(16)	5462 (9)	4790 (10)	4940 (10)	5.1 (4)
C(17)	6770 (10)	3540 (10)	4460 (10)	5.1 (4)
C(18)	7400 (10)	4580 (10)	4925 (9)	4.9 (4)
C(19)	7160 (10)	2520 (10)	4030 (10)	6.4 (4)
C(20)	8590 (10)	4910 (10)	5130 (10)	5.9 (4)
S(9)	3779 (2)	848 (2)	5653 (2)	3.76 (8)
S(10)	5266 (2)	-181 (2)	6458 (2)	3.93 (8)
C(21)	4792 (8)	135 (8)	5427 (8)	2.9 (3)
C(22)	3715 (8)	878 (8)	6872 (9)	3.4 (3)
C(23)	4377 (8)	415 (8)	7239 (9)	3.6 (3)
C(24)	2885 (9)	1425 (9)	7420 (10)	4.6 (4)
C(25)	4440 (10)	329 (9)	8260 (10)	5.1 (4)

flections had $I > 3\sigma(I)$. The variation of intensity controls (measured every hour) was less than 4.7%. 2: 4509 reflections measured ($1 \leq \theta \leq 21.5^\circ$, $\pm h$, $\pm k$, l), 4250 unique reflections (merging $R = 2.5\%$) of which 3223 reflections had $I > 3\sigma(I)$.

Structure Analysis and Refinement. Both structures were solved by a combination of direct methods and Fourier techniques and refined (full-matrix least-squares) anisotropically with hydrogen atoms (calculated ideal positions) and solvent (as found in the last Fourier difference map) included in scale factor calculations and not refined. The weighting scheme used was $1/w = (\sigma^2(I) + (0.07F_o)^2)/4F_o^2$ with $\sigma(I)$ from counting statistics. Final R , R_w , and goodness of fit values are 0.070, 0.086, and 2.00 for 1 and 0.043, 0.066, and 1.55 for 2. Scattering factors are from *International Tables for X-ray Crystallography*; all computer programs are from the Enraf-Nonius structure determination package.¹¹ The final atomic coordinates and equivalent isotropic thermal parameters are given in Tables I and II. The numbering scheme and interatomic distances for the cluster are given in Figure 1 and Table III, respectively. Both numbering scheme and interatomic distances and angles for the donor molecules are available as supplementary material (see the paragraph at the end of the paper).

Magnetic Measurements. Single-crystal ESR spectra for 1 and 2 were recorded at the Centre de Recherche Paul Pascal by using a Varian X-band spectrometer (frequency = 9.3 GHz). Susceptibility measurements were carried out on some (12.8 mg)

**Figure 1.** Numbering scheme for the cluster.**Table III. Interatomic Distances (angstroms) in the Cluster for 1 and 2^a**

atom	atom	dist	
		1	2
Nb(1)	Nb(2)	2.994	2.991
Nb(1)	Nb(2) ^b	3.009	3.000
Nb(1)	Nb(3)	2.994	2.984
Nb(1)	Nb(3) ^b	3.006	2.998
Nb(2)	Nb(3)	2.996	2.991
Nb(2)	Nb(3) ^b	2.996	2.991
Nb(1)	Cl(1)	2.450	2.445
Nb(1)	Cl(2)	2.441	2.440
Nb(1)	Cl(4)	2.444	2.447
Nb(1)	Cl(5)	2.449	2.450
Nb(1)	Cl(7)	2.543	2.535
Nb(2)	Cl(2)	2.446	2.437
Nb(2)	Cl(3)	2.444	2.443
Nb(2)	Cl(4)	2.444	2.448
Nb(2)	Cl(6)	2.445	2.441
Nb(2)	Cl(8)	2.525	2.514
Nb(3)	Cl(1)	2.445	2.437
Nb(3)	Cl(3)	2.448	2.449
Nb(3)	Cl(5)	2.449	2.440
Nb(3)	Cl(6)	2.449	2.440
Nb(3)	Cl(9)	2.533	2.530

^a ESD's are 0.001 Å and 0.003 Å for Nb-Nb and Nb-Cl distances respectively. ^b Symmetry: $-x, -y, -z$.

single crystals of 1 at the IBM Almaden Research Center with an S.H.E. Model 905 SQUID susceptometer at 50 kOe. The data were corrected for diamagnetic contributions and temperature-independent paramagnetism for the $\text{Nb}_6\text{Cl}_{18}^{3-}$ cluster ($\chi_{\text{VW}} = 0.00065 \text{ emu mol}^{-1}$ (ref 12)).

Conductivity Measurements. Ambient pressure conductivity measurements were performed for both compounds on single crystals, from room temperature to 160 K, using the standard four-probe dc technique. For the selenium salt 1, the temperature dependence of the conductivity was measured up to 7.1 kbar by using gold evaporated contacts. The isostatic-pressure-transmitting liquid was isopentane.

Band Electronic Structure Calculations. The tight-binding band electronic structure calculations¹³ were of the extended Hückel type.¹⁴ A modified Wolfsberg-Helmholz formula was used to calculate the nondiagonal $H_{\mu\nu}$ values.¹⁵ Double- ζ orbitals¹⁶

(12) Converse, J. G.; McCarley, R. E. *Inorg. Chem.* 1970, 9, 1361.
 (13) Whangbo, M.-H.; Hoffmann, R. *J. Am. Chem. Soc.* 1978, 100, 6093.

(14) Hoffmann, R. *J. Chem. Phys.* 1963, 39, 1397.

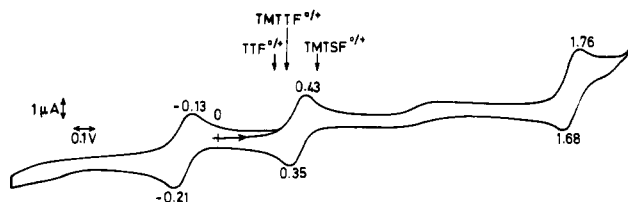


Figure 2. Cyclic voltammogram of $(\text{Et}_4\text{N})_3\text{Nb}_6\text{Cl}_{18}$ in CH_3CN (0.1 M Bu_4NPF_6) vs SCE recorded at 100 mV/s; arrows indicate the first half-wave oxidation potentials of organic donors from Table IV.

Table IV. Half-Wave Potentials of the Redox Couples for the Cluster and Selected Organic Donors

redox couple	$E_{1/2}/\text{V}^a$	solvent	electrolyte
$\text{Nb}_6\text{Cl}_{18}^{4-/3-}$	-0.17	CH_3CN	$\text{Bu}_4\text{N}^+\text{PF}_6^-$
$\text{Nb}_6\text{Cl}_{18}^{3-/2-}$	0.39	CH_3CN	$\text{Bu}_4\text{N}^+\text{PF}_6^-$
$\text{Nb}_6\text{Cl}_{18}^{2-/1-}$	1.72	CH_3CN	$\text{Bu}_4\text{N}^+\text{PF}_6^-$
$\text{TTF}^{0/+}$	0.30, ^b 0.33 ^c	CH_3CN	$\text{Et}_4\text{N}^+\text{ClO}_4^-$
$\text{TMTTF}^{0/+}$	0.27 ^c	CH_3CN	$\text{Et}_4\text{N}^+\text{ClO}_4^-$
$\text{TMTSF}^{0/+}$	0.48 ^d	CH_2Cl_2	$\text{Bu}_4\text{N}^+\text{ClO}_4^-$
	0.42	$\text{CH}_3\text{CN}:\text{CH}_2\text{Cl}_2$ (4:1)	$\text{Bu}_4\text{N}^+\text{PF}_6^-$

^a Versus standard calomel electrode. ^b Bard, A. J.; Faulkner, L. R. *Electrochemical Methods*; Wiley: New York, 1980; p 702. ^c Scott, B. A.; Kaufman; F. B.; Engler, E. M. *J. Am. Chem. Soc.* 1976, 98, 4342. ^d Lamache, M.; Wuryanto, S.; Benhamou, F. *Electrochim. Acta* 1985, 30, 817.

for C and Se were used. The exponents (ζ_μ and ζ_μ'), weighting coefficients (c_μ and c_μ') of the double- ζ orbitals, and $H_{\mu\mu}$ (electronvolts) values used were 1.831, 1.153, 0.716, 0.2630, and -21.4 for C 2s, 2.730, 1.257, 0.2595, 0.8025, and -11.4 for C 2p, 3.139, 1.900, 0.5827, 0.4846, and -20.5 for Se 4s, and 2.715, 1.511, 0.5347, 0.5553, and -13.2 for Se 4p. To reduce the computational task, the methyl groups of the TMTSF molecules were replaced by hydrogen atoms.

Results and Discussion

Electrochemical Oxidation of $\text{Nb}_6\text{Cl}_{18}^{3-}$. Previous work¹⁷ has shown that this cluster anion may occur in three different valence states n ($n = 2, 3, 4$), on the basis of magnetic^{10b,12} and spectral measurements¹⁸ and structural studies.¹⁹ Polarographic measurements in water or DMSO have been reported^{10b,20} as well as the aqueous solution electrochemistry of the analogous tantalum bromide cluster $\text{Ta}_6\text{Br}_{12}^{2+}$.²¹ The cyclic voltammogram of $[(\text{C}_2\text{H}_5)_4\text{N}]_3\text{Nb}_6\text{Cl}_{18}$ in CH_3CN was investigated to compare the redox properties of the cluster anion with those of TTF-based donors. As shown in Figure 2, the reversible $\text{Nb}_6\text{Cl}_{18}^{3-/2-}$

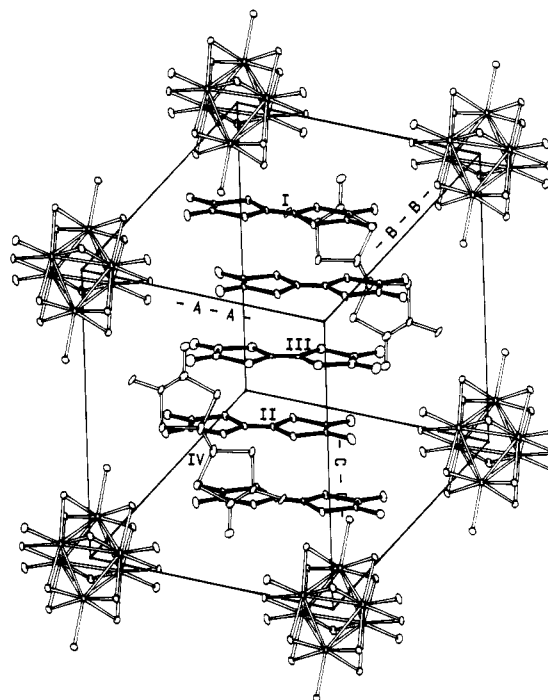


Figure 3. Projection of the unit-cell content; two clusters at corners of the unit cell have been omitted for clarity.

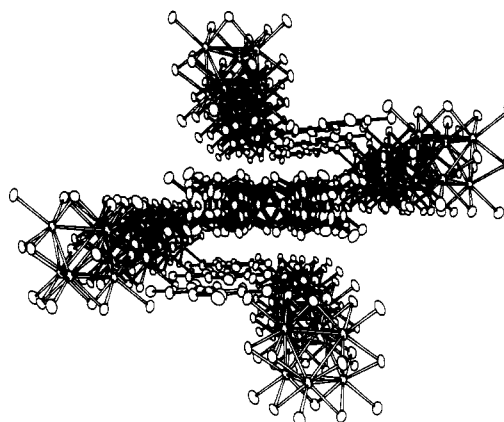


Figure 4. Perspective view along the normal to the donor planes.

couple occurs at a potential higher than those for the $\text{TTF}^{0/+}$ and $\text{TMTTF}^{0/+}$ couples (Table IV), which testifies to the possibility of electrooxidizing these donors in the presence of the ammonium salt of the trivalent cluster halide serving as electrolyte. The $\text{TMTSF}^{0/+}$ couple when measured under the actual electrocrystallization cell conditions, namely, a 4:1 $\text{CH}_3\text{CN}:\text{CH}_2\text{Cl}_2$ mixture, occurs at essentially the same potential (Table IV) as that for $\text{Nb}_6\text{Cl}_{18}^{3-/2-}$.

Extending the scan toward more anodic potentials revealed an additional quasireversible oxidation wave (Figure 2) attributed to the $\text{Nb}_6\text{Cl}_{18}^{2-/1-}$ couple ($E_{1/2} = 1.72$ V vs SCE, Table IV). This indicates that the yet unknown $\text{Nb}_6\text{Cl}_{12}^{5+}$ cluster core, a novel powerful inorganic oxidant whose potential is 0.16 V more positive than $\text{Mo}_6\text{Cl}_8^{5+}$,²² is accessible. According to well-documented calculations^{18b,23} on the electronic structure of the $\text{Nb}_6\text{Cl}_{12}^{x+}$ cluster core, the Nb-Nb bonding states in these clusters have the symmetries a_{1g} , t_{2g} , t_{1u} , and a_{2u} and can accom-

(15) Ammeter, J. H.; Bürgi, H.-B.; Thibeault, J.; Hoffmann, R. *J. Am. Chem. Soc.* 1978, 100, 3686.

(16) (a) Grant, P. M. *Phys. Rev. B* 1983, 27, 3934. (b) Emge, T. J.; Wang, H. H.; Beno, M. A.; Williams, J. M.; Whangbo, M.-H.; Evain, M. *J. Am. Chem. Soc.* 1986, 108, 8215. (c) Clementi, E.; Roetti, C. *At. Nucl. Data Tables* 1974, 14, 177.

(17) Kepert, D. L. *The early transition metals*; Academic Press: London, 1972.

(18) See, for example: (a) Schneider, R. F.; Mackay, R. A. *J. Chem. Phys.* 1968, 48, 843. Mattes, R. *Z. Anorg. Allg. Chem.* 1969, 364, 279. Fleming, P. B.; McCarley, R. E. *Inorg. Chem.* 1970, 9, 1347. Fleming, P. B.; Meyer, J. L.; Grindstaff, W. K.; McCarley, R. E. *Ibid.* 1970, 9, 1769. Fleming, P. B.; Edwards, P. A.; McCarley, R. E.; Torgeson, D. R. *Ibid.* 1972, 11, 1185. (b) Robbins, D. J.; Thomson, A. J. *J. Chem. Soc., Dalton Trans.* 1972, 2350.

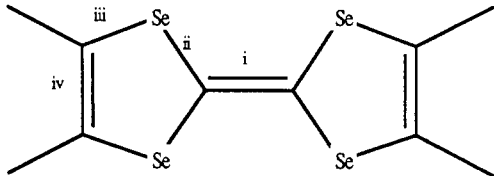
(19) (a) Simon, A.; von Schnering, H. G.; Schäfer, H. Z. *Anorg. Allg. Chem.* 1968, 361, 235. (b) Spreckelmeyer, B.; von Schnering, H. G. *Z. Anorg. Allg. Chem.* 1971, 386, 27. (c) Koknat, F. W.; McCarley, R. E. *Inorg. Chem.* 1974, 13, 295.

(20) McCarley, R. E.; Hughes, B. G.; Cotton, F. A.; Zimmerman, R. *Inorg. Chem.* 1965, 4, 1491. Eisenbraun, R.; Schäfer, H. Z. *Anorg. Allg. Chem.* 1985, 530, 222.

(21) Cooke, E. C.; Kuwana, T.; Espenson, J. *Inorg. Chem.* 1971, 10, 1081.

(22) Nocera, D. G.; Gray, H. B. *J. Am. Chem. Soc.* 1984, 106, 824.

(23) Cotton, F. A.; Haas, T. E. *Inorg. Chem.* 1964, 3, 10. Wirsich, J. *Theor. Chim. Acta* 1974, 34, 67. Simon, A. *Angew. Chem., Int. Ed. Engl.* 1988, 27, 159.

Table V. Interatomic Distances (angstroms) Averaged in *mmm* Symmetry for the Donor Molecule in 1 and in Selected TMTSF Salts from the Literature


	(TMTSF) ₅ Nb ₆ Cl ₁₈ (CH ₂ Cl ₂) _{0.5}				TMTSF ^{0a}	(TMTSF) ₂ X ^b			
	I	II	III	IV		PF ₆ ^{-c}	ClO ₄ ^{-d}	ReO ₄ ^{-e}	SiF ₅ ^{-f}
i	1.39 (2)	1.394 (14)	1.38 (2)	1.30 (3)	1.35 (1)	1.369 (14)	1.399	1.334	1.334
ii	1.873 (10)	1.864 (11)	1.868 (12)	1.91 (2)	1.892 (7)	1.875 (10)	1.868	1.882	1.885
iii	1.890 (11)	1.903 (11)	1.898 (13)	1.903 (12)	1.906 (7)	1.893 (10)	1.887	1.901	1.897
iv	1.274 (15)	1.32 (2)	1.24 (2)	1.33 (2)	1.32	1.329 (15)	1.358	1.322	1.350

^aKistenmacher, T. J.; Emge, T. J.; Shu, P.; Cowan, D. O. *Acta Crystallogr., Sect. B* 1979, 35, 772. The charge per TMTSF is 0. ^bX = PF₆⁻, ClO₄⁻, ReO₄⁻, SiF₅⁻. The charge per TMTSF is +1/2. ^cThorup, N.; Rindorf, G.; Soling, H.; Bechgaard, K. *Acta Crystallogr., Sect. B* 1981, 37, 1236. ^dRindorf, G.; Soling, H.; Thorup, N. *Acta Crystallogr., Sect. B* 1982, 38, 2805. ^eRindorf, G.; Soling, H.; Thorup, N. *Acta Crystallogr., Sect. C* 1984, 40, 1137. ^fEriks, K.; Beno, M. A.; Bechgaard, K.; Williams, J. M. *Acta Crystallogr., Sect. C* 1984, 40, 1715.

modate 16 electrons. Therefore, oxidation from Nb₆Cl₁₂²⁺ to Nb₆Cl₁₂⁴⁺ has emptied the totally symmetrical, slightly bonding a_{2u} orbital and Nb₆Cl₁₂⁵⁺ is a paramagnetic 13-electron cluster since one electron has been removed from the bonding t_{1u} orbital.²⁴ At present, we are attempting to characterize this oxidized cluster. The reversibility suggests that the corresponding monoanion should be chemically accessible.

Structure Description. As expected from the similarity in their unit-cell parameters, the charge-transfer salts 1 and 2 are isostructural. Their dominant structural feature is the presence of an organic stack parallel to the *c* axis (Figure 3) and built up from a TMTSF (respectively TMTTF) molecule (I) centered at (1/2, 1/2, 0), a second TMTSF molecule (II) in general position (*z* = 0.734) and a third molecule (III) centered at (1/2, 1/2, 1/2). The organic stack is surrounded by Nb₆Cl₁₈³⁻ cluster anions at the origin of the cell. An additional TMTSF molecule (IV), orthogonal to the stack, is located on the (010) plane. Solvent molecules are detected albeit poorly refined in a cavity centered at the middle of the (100) plane.

The perspective view along the normal to the plane of the intrastack TMTSF molecules (Figure 4) exemplifies the one-dimensional character of the structure and the relative positions of the donor stack, the type IV donor molecules, and inorganic cluster columns. The organic stack is surrounded by four such columns, and no direct face-to-face interstack Se...Se or S...S interaction occurs, unlike in the Bechgaard salt series.²⁵ Note also the offsets of the inorganic anion centroids from the pseudosymmetry planes of the organic stack motif (2.37 and 2.42 Å vs the horizontal and vertical planes, respectively, in Figure 4).

Figure 5 displays a 90° rotation of Figure 4 along the TMTSF long molecular axis. Specifically, Figure 5 is a projection onto the symmetry plane of the intrastack TMTSF (I, II, III) central C=C bonds. This view emphasizes the pattern of intrastack molecular overlap, bearing in mind that the clusters at the left and right of the stack lie respectively slightly above and below the projection plane. The flat TMTSF (respectively TMTTF) units are almost perpendicular to the long unit-cell axis *c* and are stacked with four molecules per unit cell along this axis, which is also the direction of high electrical conductivity (vide supra). Within a stack, an inversion occurs at every other unit leading to an unprecedented

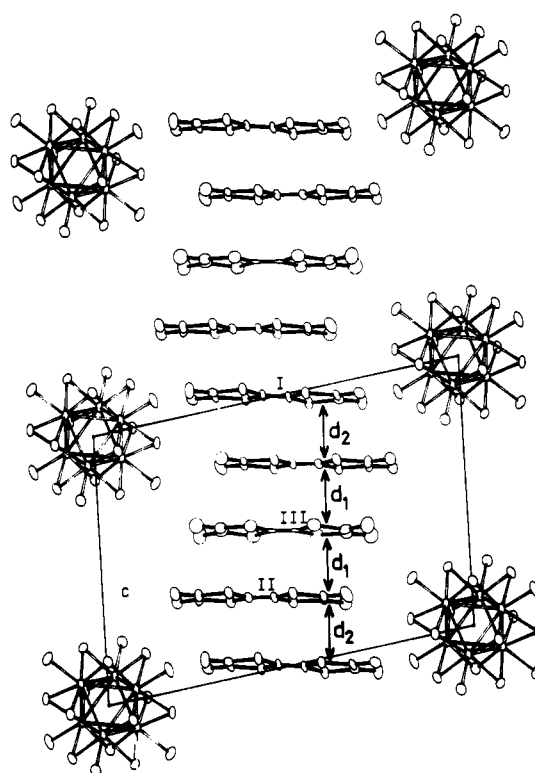
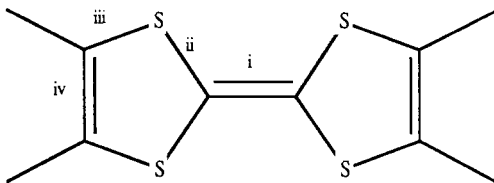


Figure 5. A 90° rotation of Figure 4 with two stacks of clusters omitted for clarity (see text).

sequence of overlap displacements. Indeed, along the molecular axis, the overlap displacements do not simply alternate ("zigzag" stacking mode) as in the Bechgaard salts.²⁵ They instead successively alternate and slip in such a way that the stacking units and the cluster halides become neatly interlaced. There are two crystallographically independent, essentially identical interplanar distances ($d_1 = 3.62$ and $d_2 = 3.66$ Å for 1, $d_1 = 3.55$ Å and $d_2 = 3.59$ Å for 2, Figure 5). Figure 6 displays the shortest intrastack selenium-selenium and sulfur-sulfur contacts. These distances reflect some irregularity of the stacking periodicity, thus suggesting that the repetition of trimers (II-III-II) and monomers (I) occurs along the stack. Finally, it is worth noting that the stacking parameters *c* for 1 and 2 are essentially twice those of the (TMTSF)₂X and (TMTTF)₂X salts, respectively (14.581/2 = 7.290 Å and 14.334/2 = 7.167 Å to be compared to 7.297 for (TMTSF)₂PF₆²⁶ and 7.112 for (TMTTF)₂BF₄²⁷), further

(24) Saillard, J.-Y., private communication.

(25) Thorup, G.; Rindorf, G.; Soling, H.; Johannsen, I.; Mortensen, K.; Bechgaard, K. *J. Phys. (Oxford)* 1983, 44, C3-1017.

Table VI. Interatomic Distances (angstroms) Averaged in *mmm* Symmetry for the Donor Molecule in 2 and in Selected TMTTF Salts from the Literature


	(TMTTF) ₅ Nb ₆ Cl ₁₈ (CH ₂ Cl ₂) _{0.5}				(TMTTF) ₂ X ^a			
	I	II	III	IV	Br ^{b,f}	BF ₄ ^{-c,f}	SCN ^{-d,f}	Mo ₆ Cl ₁₄ ^{2-e,g}
i	1.37 (2)	1.373 (12)	1.40 (2)	1.33 (2)	1.345	1.390 (12)	1.381 (10)	1.379 (4)
ii	1.740 (8)	1.724 (9)	1.714 (13)	1.755 (11)	1.739	1.717 (3)	1.738 (2)	1.715 (3)
iii	1.761 (9)	1.749 (9)	1.726 (12)	1.751 (11)	1.754	1.735 (3)	1.775 (2)	1.737 (3)
iv	1.330 (12)	1.349 (12)	1.349 (15)	1.323 (14)	1.323	1.353 (10)	1.333 (6)	1.347 (5)

^aX = Br⁻, BF₄⁻, SCN⁻, Mo₆Cl₁₄²⁻. ^bGaligné, J. L.; Liautard, B.; Peytavin, S.; Brun, G.; Fabre, J. M.; Toreilles, E.; Giral, L. *Acta Crystallogr., Sect. B* 1978, 34, 620. ^cGaligné, J. L.; Liautard, B.; Peytavin, S.; Brun, G.; Maurin, M.; Fabre, J. M.; Toreilles, E.; Giral, L. *Acta Crystallogr., Sect. B* 1979, 35, 1129. ^dGaligné, J. L.; Liautard, B.; Peytavin, S.; Brun, G.; Maurin, M.; Fabre, J. M.; Toreilles, E.; Giral, L. *Acta Crystallogr., Sect. B* 1979, 35, 2609. ^eOuahab, L.; Batail, P.; Perrin, C.; Garrigou-Lagrange, C. *Mater. Res. Bull.* 1986, 21, 1223. ^fThe charge per TMTTF is +1/2. ^gThe charge per TMTTF is +1.

Table VII. Comparison of Relevant Intracluster Parameters Averaged in *O_h* Symmetry for Nb₆Cl₁₈ⁿ⁻ salts

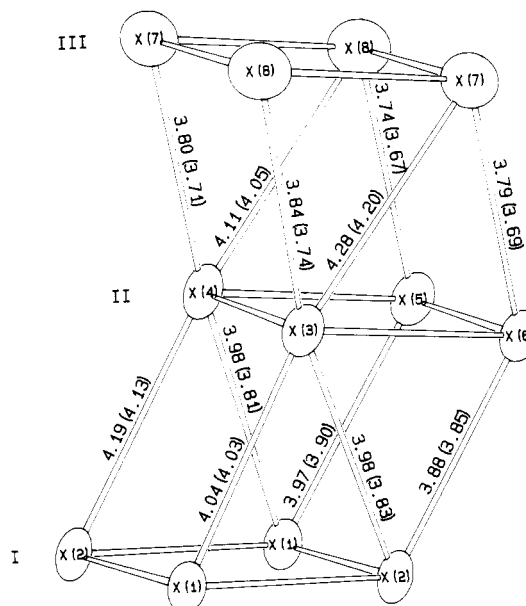
compound	cluster electron count	d _{Nb-Nb} , Å	d _{Nb-Cl_b} , Å	d _{Nb-Cl_t} , Å	d _{c-Nb} ^a , Å	d _{c-Cl_b} ^a , Å	d _{c-Cl_t} ^a , Å	d _{nb-Cl_bplane} ^b , Å	Cl _b -Nb-Cl _b , deg	Nb-Cl _b -Nb, deg
(PyH) ₂ Nb ₆ Cl ₁₈ ^c	14	3.045 (9)	2.433 (18)	2.475 (18)	2.153 ^d	3.420 ^d	4.628 ^d		167.37 ^d	77.46 ^d
(Ph ₃ AsOH) ₂ Nb ₆ Cl ₁₈ ^e	14	3.016 (6)	2.42 (1)	2.48 (1)	2.13 ^d	3.395 ^d	4.613 ^d		167.12 ^d	77.2 (5)
(Me ₄ N) ₂ Nb ₆ Cl ₁₈ ^f	14	3.018 (2)	2.418 (6)	2.457 (3)	2.13	3.40	4.59	0.27	167.21 (7)	77.2 (3)
(Me ₄ N) ₃ Nb ₆ Cl ₁₈ ^g	15	2.967 (17)	2.43 (5)	2.52 (3)	2.10	3.40	4.61	0.31	165.4 (18)	75.4 (17)
LuNb ₆ Cl ₁₈ ^h	15	2.956 (2)	2.432 (4)	2.623 (2)	2.090 ^d	3.408 ^d	4.712 ^d	0.32	164.83 ^d	74.86 ^d
(TMTSF) ₅ Nb ₆ Cl ₁₈ ⁻	15	2.999 (6)	2.446 (3)	2.534 (7)	2.120 (3)	3.432 (5)	4.653 (9)	0.306 (4)	165.6 (2)	75.6 (2)
(CH ₂ Cl ₂) _{0.5}										
(TMTTF) ₅ Nb ₆ Cl ₁₈ ⁻	15	2.993 (5)	2.443 (4)	2.526 (9)	2.116 (3)	3.427 (5)	4.64 (1)	0.308 (6)	165.5 (3)	75.5 (2)
(CH ₂ Cl ₂) _{0.5}										
(TTF) ₂ (Et ₄ N)Nb ₆ Cl ₁₈ ⁻	15	2.984 (5)	2.443 (6)	2.518 (4)	2.110 (3)	3.426 (3)	4.631 (1)	0.313 (4)	165.3 (2)	75.29 (6)
(CH ₃ CN) ⁱ										
K ₄ Nb ₆ Cl ₁₈ ^j	16	2.91 (5)	2.48 (2)	2.60 (3)	2.06 ^d	3.46 ^d	4.67 ^d	0.39 ^d	161.9 ^d	71.9 ^d
CsLuNb ₆ Cl ₁₈ ^k	16	2.913 (2)	2.445 (3)	2.667 (1)	2.060 ^d	3.420 ^d	4.727 ^d	0.36	163.11 ^d	73.13 ^d
KGdNb ₆ Cl ₁₈ ^l	16	2.918 (2)	2.455 (4)	2.648 (1)	2.062 ^d	3.428 ^d	4.716 ^d	0.36	162.98 ^d	73.00 ^d
KLuNb ₆ Cl ₁₈ ^h	16	2.916 (2)	2.452 (3)	2.654 (1)	2.063 ^d	3.433 ^d	4.711 ^d	0.36	162.89 ^d	72.90 ^d

^aDistance from center of cluster to indicated atom. ^bDistance from niobium atom to plane formed by four nearest bridging Cl atoms. ^cSpreckelmeyer, B.; von Schnering, H. G. *Z. Anorg. Allg. Chem.* 1971, 386, 27. ^dCalculated from the corresponding reference. ^eField, R. A.; Kepert, D. L.; Robinson, B. W.; White, A. H. *J. Chem. Soc., Dalton Trans.* 1973, 1858. ^fKoknat, F. W.; McCarley, R. E. *Inorg. Chem.* 1972, 11, 812. ^gKoknat, F. W.; McCarley, R. E. *Inorg. Chem.* 1974, 13, 295. ^hIhmaine, S.; Perrin, C.; Peña, O.; Sergent, M. *J. Less-Common Met.* 1988, 137, 323. ⁱReference 7. ^jSimon, A.; von Schnering, H. G.; Schafer, H. *Z. Anorg. Allg. Chem.* 1968, 361, 235. ^kIhmaine, S.; Perrin, C.; Sergent, M. *Acta Crystallogr., Sect. C* 1989, 45, 705. ^lIhmaine, S.; Perrin, C.; Sergent, M. *Acta Crystallogr., Sect. C* 1987, 43, 813.

emphasizing the similarity of the stacking patterns.

The bond distances for the four independent donor molecules are averaged in *D_{2h}* symmetry and compared in Tables V and VI for 1 and 2, respectively, with corresponding distances for a variety of oxidation states of the donors. For both compounds, molecule IV significantly differs from the other three. The set of characteristic bonds for IV are similar to those of a neutral donor, while geometries for I, II, and III are essentially identical and typical of charged species. We can then suggest that molecule IV is neutral, whereas the four molecules of type I, II, and III share the three positive charges. Our calculations for the isolated molecules I-IV are in agreement with this analysis. The HOMOs of I, II, and III all lie within a narrow 0.15-eV energy range, whereas that of molecule IV lies about 0.4 eV below.

The intracluster bond distances are given in Table III for both compounds. Related average distances and angles are compared in Table VII with those reported for a series

**Figure 6. Intracluster Se...Se (S...S) distances (angstroms) in 1 (X = Se) and 2 (X = S).**

(26) Thorup, G.; Rindorf, G.; Soling, H.; Bechgaard, K. *Acta Crystallogr., Sect. B* 1981, 37, 1236.

(27) Galigné, J. L.; Liautard, B.; Peytavin, S.; Brun, G.; Maurin, M.; Fabre, J.; Toreilles, E.; Giral, L. *Acta Crystallogr., Sect. B* 1979, 35, 1129.

Table VIII. Shortest (<4 Å) X•••Cl Donor Chalcogen-Chloride Contacts (X = Se for 1, X = S for 2)

atom	atom	dist/Å	
		1	2
X(1)	Cl(4)	3.766	3.729
X(1)	Cl(7)	3.827	
X(4)	Cl(4)	3.692	3.725
X(4)	Cl(8)	3.368	3.330
X(5)	Cl(5)	3.812	3.981
X(5)	Cl(6)	3.638	3.598
X(7)	Cl(8)		3.834
X(8)	Cl(6)	3.727	3.677
X(10)	Cl(8)	3.691	3.793

Table IX. Cl•••H Contacts (angstroms) <3 Å and Corresponding Cl•••H-C Angles (degrees) for 1 and 2

atom	atom	dist		angle	
		1	2	1	2
Cl(1)	H(26)	2.59	2.78	167.3	167.7
Cl(5)	H(6)		2.98		143.4
Cl(7)	H(1)	2.87	2.84	167.5	164.3
Cl(8)	H(10)	2.92	2.91	151.5	128.7
Cl(8)	H(28)	2.73	2.73	170.1	172.3
Cl(9)	H(20)		2.73		159.3
Cl(9)	H(24)		2.86		157.1

of closed-shell cation salts of niobium cluster halides with different electron counts.

The characteristic distances and angles are as expected for a 15-electron cluster core in 1 and 2, except for the niobium-niobium bond lengths. The latter are unusually long and actually intermediate between those reported for $\text{Nb}_6\text{Cl}_{12}^{3+}$ and $\text{Nb}_6\text{Cl}_{12}^{4+}$ with formal cluster electron counts of 15 and 14, respectively.

According to Koknat and McCarley's exhaustive description^{19c} of the influence of oxidation on the structure of the $\text{Nb}_6\text{Cl}_{12}^{x+}$ cluster core, the major effect comes from the removing of electrons from the metal-based bonding orbital a_{2u} , which causes a regular increase of the Nb-Nb bond distances. As a result, each niobium atom moves up toward the plane of its four bridging chlorine atom (Cl_b) neighbors, which lessens the bridging chlorine...terminal chlorine (Cl_t) steric hindrance and enables the Cl_t atoms to get closer to the metals. A secondary effect is a concomitant strengthening of the Nb- Cl_t bonds ionicity.^{19c} These two effects account for the observed net shrinkage of the Nb- Cl_t bonds upon oxidation of the cluster core while the Nb- Cl_b bonds remain unaffected (Table VII). Indeed, in the present charge-transfer salts the Nb- Cl_t bonds and the Cl_b -Nb- Cl_b and Nb- Cl_b -Nb angles are normal (Table VII) for $\text{Nb}_6\text{Cl}_{12}^{3+}$. Therefore, in 1 and 2, the observed slight expansion of the cluster envelope (exemplified by longer c-Cl distances from the center (c) of the cluster to the outer chlorine atoms) is attributed to an increase of the Nb-Nb bond lengths only.⁷

Finally, the binding of the organic and inorganic subsystems in such that a set of chalcogen-chloride (Table VIII) and C-H...Cl (Table IX) intermolecular contacts are identified. Note in particular that the Se(4)...Cl(8) (3.368 Å) and S(4)...Cl(8) (3.330 Å) distances are much shorter than the corresponding van der Waals separations of 3.80 and 3.65 Å.

Charge Balance, Mixed-Valency, and Electrical Conductivity. The analysis of the crystal and molecular electronic structure of the salts indicates the presence of an organic stack comprising four partially oxidized donor molecules per trivalent cluster anion and an additional neutral donor whose molecular plane is orthogonal to those of the cation radicals in the stack (at angles of 88.8, 87.8, and 89.3° with respect to I, II, and III respectively). This

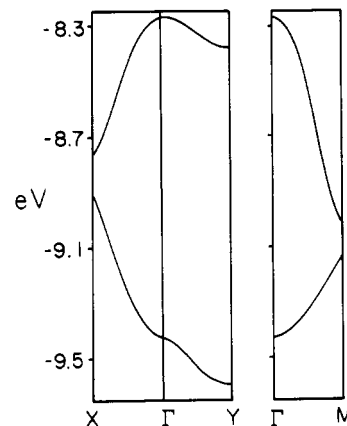


Figure 7. Band structure for the $(\text{TMTSF})_2$ slabs in $(\text{TMTSF})_2\text{PF}_6$.²⁶ Γ , X, Y and M refer to the wave vectors (0, 0), $(a^*/2, 0)$, $(0, b^*/2)$, and $(-a^*/2, b^*/2)$, respectively.

situation is reminiscent of that reported for $(\text{HMTTeF})_4(\text{PF}_6)_2$,²⁸ and the formulation of the salts is properly expressed as $(\text{D}_4)^{3+}(\text{D}^0)(\text{Nb}_6\text{Cl}_{18})^{3-}$ (D = TMTSF, 1; TMTTF, 2). Hence, the band filling amounts to $5/8$ since three electrons are taken away out of a total of eight required to fill up the bonding combinations of the HOMO's of the four intrastack molecules. Since only five electrons are left to fill the four bands of the donor chains, the third band should be half-filled. Consequently, one might expect that 1 and 2 would behave as metals.

This is in contradiction with the electrical conductivity results for both compounds since four-probe single-crystal resistivity measurements indicate an activated behavior between 160 and 280 K. The activation energies are 0.16 and 0.20 eV for 1 and 2, respectively. Below 160 K, the sample resistances were too large to be measured. The room-temperature conductivity is $0.5 \Omega^{-1} \text{cm}^{-1}$ for 1.

In both compounds, the large cluster anions are related by the unit-cell axis translations. This leaves them very much further apart than in any other salt of the same cluster anion with small, monoatomic inorganic or metal cations. For example, the close-packed separation is only 9.22 Å in $\text{LuNb}_6\text{Cl}_{18}$.²⁹ Although the crystal packing appears to be reasonably tight (vide infra), resistivity measurements have been conducted for 1 at high hydrostatic pressures in order to assess the actual stiffness of these organic-inorganic hybrids and eventually suppress the observed electron localization. Preliminary experiments indicate that the activated nature of the ambient pressure conductivity is maintained up to 7.7 kbar.

Band Electronic Structure. In an attempt to understand the contrasting electrical properties of the $(\text{TMTSF})_2$ and $(\text{TMTTF})_5\text{Nb}_6\text{Cl}_{18}(\text{CH}_2\text{Cl}_2)_{0.5}$ salts 1 and 2 and the Bechgaard salts $(\text{TMTSF})_2\text{X}$ (X = PF_6^- , ClO_4^- , ...),³⁰ we performed tight-binding band electronic structure calculations on the cationic sublattices of $(\text{TMTSF})_2\text{PF}_6$ and $(\text{TMTSF})_5\text{Nb}_6\text{Cl}_{18}(\text{CH}_2\text{Cl}_2)_{0.5}$. We note that in the case of the latter salt 1, there are several short Se...Se contacts (3.66, 3.85, 3.88 Å) between molecule IV and the stack, which could lead to some interstack coupling. The dispersion relations for the two TMTSF slabs are shown in Figures 7 and 8. It is clear from Figure 7 that the TMTSF sublattice of the PF_6 salt is a quasi-1D system

(28) Kikuchi, K.; Yakushi, K.; Kuroda, H.; Ikemoto, I.; Kobayashi, K.; Honda, M.; Katayama, C.; Tanaka, J. *Chem. Lett.* **1985**, *4*, 419.

(29) Ihmame, S.; Perrin, C.; Peña, O.; Sergent, M. *J. Less Common Met.* **1988**, *137*, 323.

(30) Bechgaard, K.; Jacobsen, C. S.; Mortensen, K.; Pedersen, H. J.; Thorup, N. *Solid State Commun.* **1980**, *33*, 1119.

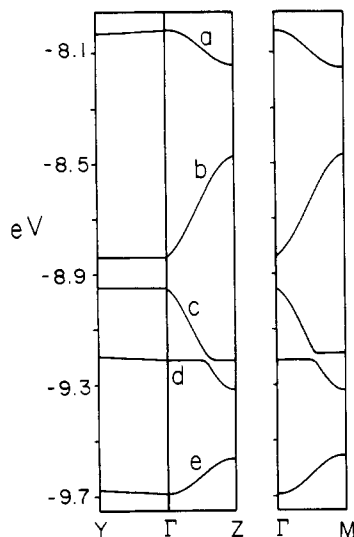


Figure 8. Band structure for the $(\text{TMTSF})_5$ slabs in $(\text{TMTSF})_5\text{Nb}_6\text{Cl}_{18}(\text{CH}_2\text{Cl}_2)_{0.5}$. Γ , Y, Z, and M refer to the wave vectors $(0, 0)$, $(b^*/2, 0)$, $(0, c^*/2)$, and $(-b^*/2, c^*/2)$, respectively.

with *nonnegligible* interstack interactions.³¹ This is in contrast with the case of the $\text{Nb}_6\text{Cl}_{18}$ salt 1 (Figure 8), which shows a *perfect 1D band structure*. With seven electrons to fill the HOMO bands of Figure 8, band b is half-filled. The dispersion of this band is relatively modest (0.37 eV) compared with that of the half-filled upper band of Figure 7, which shows a dispersion of 0.80 eV. Nevertheless, the *total width* of the HOMO bands in both salts are comparable. Consequently, from the viewpoint of the one-electron band structure of the cation sublattice alone, there is no reason why the present salt 1 should exhibit the activated behavior typical of localized systems. Further work is needed to understand this interesting question. Nevertheless, we would like to point out that whereas all TMTSF molecules in the PF_6 salt are subject to the same anionic potential, this is not the case in 1 (see Figures 3 and 5). This could provide a driving force for the localization.

Since the structural analysis indicates a succession of trimers II-III-II and monomers I along the stack, the question arises of how this structural feature is related to the actual electronic structure, i.e., the nature of the five bands of Figure 8. Bands a and e have the character of type II and III molecules with a smaller contribution of type I molecule. Band d, which undergoes a slightly avoided crossing with band c, has almost exclusively the character of the type IV molecule. Bands b and c have the character of type I and II molecules with a small participation of type III molecule. Thus, one can think of the localized electrons of the stacks in 1 as unpaired electrons sitting on trimeric units II-I-II only weakly interacting through type III molecule. In other words, the donor stacks can be formally considered as a series of trimeric and monomeric units, and the nature of both units is different, depending upon structural or electronic viewpoints.

The link between those two descriptions is readily apparent on the basis of the calculated interaction energies (β)³³ for the HOMOs of the different TMTSF molecules.

(31) These results are in good agreement with previous theoretical^{32a,b} and optical^{32c} results.

(32) (a) Grant, P. M. *J. Phys. (Orsay)* **1983**, *44*, C3-847. (b) Whangbo, M.-H.; Walsh, W. M.; Haddon, R. C.; Wudl, F. *Solid State Commun.* **1982**, *43*, 637. (c) Jacobsen, C. S.; Tanner, D. B.; Bechgaard, K. *J. Phys. (Orsay)* **1983**, *44*, C3-859.

Table X. Room Temperature Characteristics of the ESR Signal for 1 and 2 in Three Orthogonal Directions

g	$(\text{TMTSF})_5\text{Nb}_6\text{Cl}_{18}(\text{CH}_2\text{Cl}_2)_{0.5}$			$(\text{TMTTF})_5\text{Nb}_6\text{Cl}_{18}(\text{CH}_2\text{Cl}_2)_{0.5}$		
	1.979	1.976	1.963	1.978	1.982	1.980
$\Delta H/G$	90	65	60	16.5	17	16

The interaction energy between orbitals i and j (β_{ij}) can be written as (1), where $c_{\nu i}$ denotes the coefficient of atomic

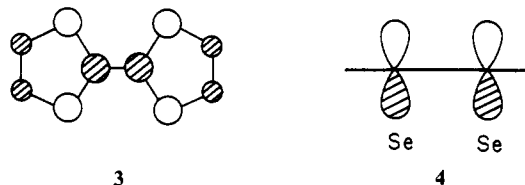
$$\beta_{ij} = \sum_{\nu} \sum_{\mu} c_{\nu i} c_{\nu j} \langle \chi_{\nu} | H^{\text{eff}} | \chi_{\mu} \rangle \quad (1)$$

orbital χ_{ν} in the molecular orbital Ψ_i (2). These interaction

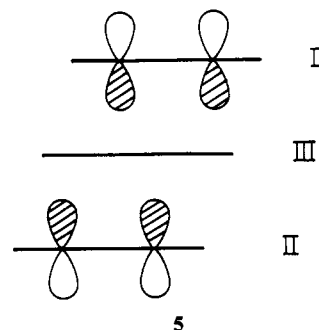
$$\Psi_i = \sum_{\nu} c_{\nu} \chi_{\nu} \quad (2)$$

energies have been extensively used by Whangbo et al.^{33a} to discuss the electronic structure of molecular conductors. There are two different interaction types in the chain of the $\text{Nb}_6\text{Cl}_{18}$ salt 1: I-II and II-III (see Figure 5). Their interaction energies ($\beta_{\text{I-II}}^{\text{HOMO-HOMO}}$ and $\beta_{\text{II-III}}^{\text{HOMO-HOMO}}$) are 0.460 and 0.769 eV, respectively. The corresponding interaction energies in the stack of the PF_6 salt are much more similar: 0.440 and 0.537 eV.

Since the II-III interaction is appreciably stronger, we can consider the $(\text{TMTSF})_4$ stack as being built from trimers II-III-II and monomers I. When constructing the levels of the trimeric unit from the HOMOs of each molecule, it is convenient to represent the HOMO of TMTSF (3) by the simplified side view 4. One of the two



combinations of the $\Psi_{\text{II}}^{\text{HOMO}}$'s interacts strongly with $\Psi_{\text{III}}^{\text{HOMO}}$ leading to high- and low-lying combinations. These bonding and antibonding combinations will be the major components of bands a and e. The second combination of the $\Psi_{\text{II}}^{\text{HOMO}}$'s (5) cannot interact by symmetry



with $\Psi_{\text{III}}^{\text{HOMO}}$ and stays at the same energy as $\Psi_{\text{II}}^{\text{HOMO}}$. The band orbitals of the stack can now be built from the Bloch functions associated with the orbitals of the trimeric

(33) (a) Whangbo, M.-H.; Williams, J. M.; Leung, P. C. W.; Beno, M. A.; Emge, T. J.; Wang, H. H. *Inorg. Chem.* **1985**, *24*, 3500. Williams, J. M.; Wang, H. H.; Emge, T. J.; Geiser, U.; Beno, M. A.; Leung, P. C. W.; Carlson, K. D.; Thorn, R. J.; Schultz, A. J.; Whangbo, M.-H. *Prog. Inorg. Chem.* **1987**, *35*, 51. (b) Since overlap is explicitly included in extended Hückel calculations, these interaction energies (β) should not be confused with the conventional transfer integrals (t). Although the two quantities are obviously related and have the same physical meaning, they will coincide only under neglect of overlap.

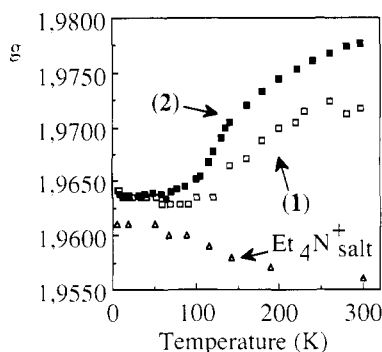


Figure 9. Temperature dependence of the g value for single crystals of 1 and 2 and for a powder of $(\text{Et}_4\text{N})_3\text{Nb}_6\text{Cl}_{18}$; for the selenated salt 1 presenting an anisotropic signal at room temperature (see Table X), the measurements were performed for an orientation corresponding to $g = 1.972$ and $\Delta H = 64$ G at 295 K.

unit and $\Psi_{\text{I}}^{\text{HOMO}}$. Due to the good energy match, $\Psi_{\text{I}}^{\text{HOMO}}$ mixes preferentially with 5. This leads to two bands (b and c) with strong $\Psi_{\text{I}}^{\text{HOMO}}$ and $\Psi_{\text{II}}^{\text{HOMO}}$ character. Band b (i.e., the half-filled one) represents the antibonding combinations of $\Psi_{\text{I}}^{\text{HOMO}}$ and 5 along the chain. The symmetry constraints are definitely weaker in the $(\text{TMTSF})_4$ stack, so that some of the $\Psi_{\text{III}}^{\text{HOMO}}$ can mix into the b band, but the local symmetry effect is strong enough to keep its contribution weak.

ESR and SQUID Magnetometer Measurements.

For both compounds, a single Lorentzian line is observed by electron spin resonance between 5 and 300 K. The g eigenvalues were deduced from the measurements of the ESR signal in six different orientations. The results are not very accurate because the crystals are small. Moreover, small differences were found among different samples. A summary of the data is given in Table X. The signal is quasiisotropic for the TMTTF salt but largely anisotropic in the case of the TMTSF salt. The temperature dependence of the g factors is displayed Figure 9, which also gives as a reference for the cluster-only value¹² the variation of the g factor for a powder sample of $(\text{Et}_4\text{N})_3\text{Nb}_6\text{Cl}_{18}$. Below ca. 100 K, the g values for 1 and 2 are essentially constant and identical (1.964) and slightly larger than the cluster-only value (1.961). At temperatures above 100 K, the g factor of the charge-transfer salts and of the tetraethylammonium salt present opposite variations. Similarly, the temperature variation of the peak-to-peak line width of 1 and 2 are comparable and different from that of $(\text{Et}_4\text{N})_3\text{Nb}_6\text{Cl}_{18}$ (Figure 10).

The reciprocal susceptibility of 1 investigated between 300 and 6 K (Figure 11) slightly saturates near room-temperature, indicating the onset of the Pauli susceptibility of delocalized electrons as discussed below. For $\text{Nb}_6\text{Cl}_{18}^{3-}$, the previously determined¹² temperature-independent paramagnetism (TIP) value of $650 \times 10^{-6} \text{ emu mol}^{-1}$ was introduced as an additive constant in the fitting, and this was found to be satisfactory. The Curie-Weiss fit [$\chi = C/(T + \theta)$] of the data for temperatures below 40 K gave a value of $\theta = 0.8$ K for 1 and an effective magnetic moment value of ca. $1.69 \mu_{\text{B}}$. The latter is close to the spin-only value ($\mu = 1.73 \mu_{\text{B}}$) for one localized unpaired electron. This further confirms the formulation with molecule IV being neutral.

1 and 2 are composed of two magnetically active subsystems, namely, the paramagnetic 15-electron niobium cluster anion and the organic radical cation stack, D_4^{3+} ($\text{D} = \text{TMTSF}$ or TMTTF). In the absence of magnetic interaction between the two systems, one expects either two distinct resonance lines or a single one characteristic of one

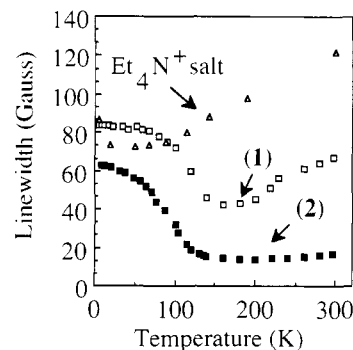


Figure 10. Temperature dependence of the ESR line width for single crystals of 1 and 2 and for a powder of $(\text{Et}_4\text{N})_3\text{Nb}_6\text{Cl}_{18}$; for 1 the measurements were performed for an orientation corresponding to $g = 1.972$ and $\Delta H = 64$ G at 295 K.

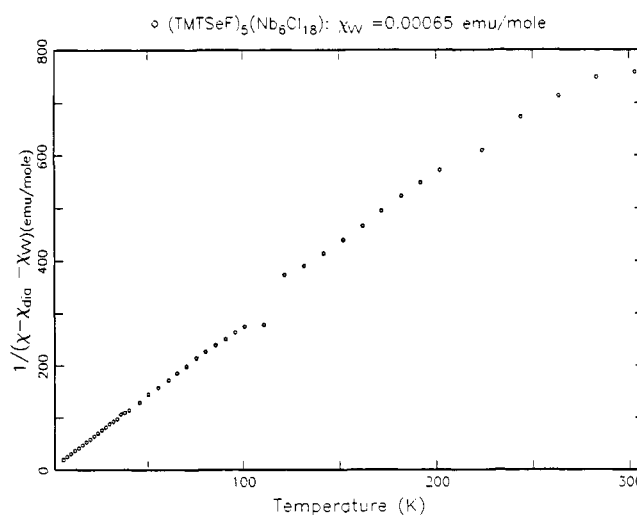


Figure 11. Reciprocal magnetic susceptibility corrected for diamagnetism and temperature-independent paramagnetism (van Vleck term) as a function of temperature for the TMTSF salt 1. (The net susceptibility for the data at ca. 110 K was essentially on the order of the error bar, the sample susceptibility being compensated by the sample holder diamagnetic contribution.)

of the two subsystems only. In the latter case, one of the resonances cannot be observed because of a very weak signal or a rapid relaxation. Since the g values for TMTSF^{2+} and TMTTF^{2+} range between 1.990–2.045³⁴ and 2.002–2.012,³⁵ respectively, it can be seen in Figure 9 that the single resonances observed for 1 and 2 are in fact admixtures of the two subsystem resonances. Therefore, this demonstrates that the organic spins of the donors chains and the inorganic cluster spins are interacting. Similar situations have been reported for example for *p*-phenylenediamine-chloranil,³⁶ TTF-TCNQ,³⁷ (perylene)₂[Pd(mnt)₂],³⁸ Cu(dpa)(TCNQ)₂,³⁹ and Cu(pc)I.⁴⁰ In

(34) Kinoshita, N.; Tokumoto, M.; Anzai, H.; Ishiguro, T.; Saito, G.; Yamabe, T.; Teramae, H. *J. Phys. Soc. Jpn.* **1984**, *53*, 1504.

(35) Onoda, M.; Nagasawa, H.; Kobayashi, K. *J. Phys. Soc. Jpn.* **1985**, *54*, 1240.

(36) Hughes, R. C.; Soos, Z. G. *J. Chem. Phys.* **1968**, *48*, 1066.

(37) (a) Gulley, J. E.; Weiher, J. F. *Phys. Rev. Lett.* **1975**, *34*, 1061. (b) Tomkiewicz, Y.; Taranko, A. R.; Torrance, J. B. *Phys. Rev. Lett.* **1976**, *36*, 751.

(38) Alcácer, L.; Maki, A. H. *J. Phys. Chem.* **1976**, *80*, 1912.

(39) Inoue, M.; Inoue, M. B. *Inorg. Chem.* **1986**, *25*, 37.

(40) Ogawa, M. Y.; Martinsen, J.; Palmer, S. M.; Stanton, J. L.; Tanaka, J.; Greene, R. L.; Hoffman, B. M.; Ibers, J. A. *J. Am. Chem. Soc.* **1987**, *109*, 1115.

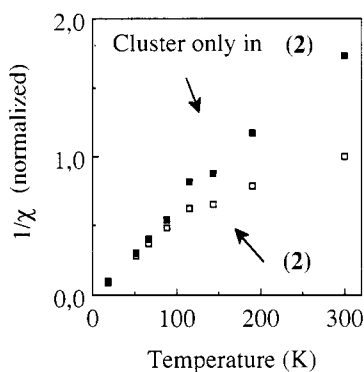


Figure 12. Reciprocal normalized spin susceptibility for the TMTTF salt 2 and for the cluster only in 2 as calculated by using the g decomposition technique (see text).

such cases where the ESR absorptions merge into one line, a susceptibility-weighted g value⁴¹ is expressed

$$g_{\text{obs}} = \alpha_a g_a + \alpha_c g_c \quad (3)$$

in which α_a and α_c are the fractional spin susceptibilities:

$$\alpha_a = \chi_a / (\chi_a + \chi_c)$$

$$\alpha_c = \chi_c / (\chi_a + \chi_c)$$

and χ_a and χ_c the individual susceptibilities for the anion and the radical cation chain, respectively. The individual susceptibilities χ_a and χ_c are readily obtained⁷ from eq 3, providing g_a , g_c , and the total susceptibility χ_{obs} ($=\chi_a + \chi_c$) are known over the whole range of temperature.

The application of a similar g decomposition technique to the estimation of the individual spin susceptibilities was hampered in the case of 1 since the g value of TMTSF^{•+} is angularly dependent³⁴ and our experiments have been performed in an arbitrary orientation relative to the crystal axis. On the other hand, the g value of TMTTF^{•+} is only slightly dependent upon orientation (2.012–2.002³⁵) and the g tensor components are essentially temperature independent. Hence, given a constant $g = 2.008$ for TMTTF^{•+}, the observed cluster-only variation with temperature of the g factor for $(\text{Et}_4\text{N})_3\text{Nb}_6\text{Cl}_{18}$ (Figure 9), and the normalized total spin susceptibility displayed in Figure 12, we were able to carry out the signal decomposition and estimate the cluster susceptibility in 2. The cluster-only spin susceptibility is accounted for by a Curie law characteristic of localized noninteracting spins.

The organic chain susceptibility obtained by the same procedure is essentially constant for temperatures above 150 K⁴² as observed in the $(\text{TMTTF})_2\text{X}$ series⁴³ ($\text{X} = \text{BF}_4^-$,

ClO_4^- , PF_6^- , ...). This is the characteristic behavior for a delocalized electron gas with strong correlations as is consistent with the observation of activated conductivities for 1 and 2.⁴⁴ Finally, it should be noted that $(\text{TTF})_2\text{-(Nb}_6\text{Cl}_{18})(\text{Et}_4\text{N})(\text{CH}_3\text{CN})^7$ presents a similar Curie-like total spin susceptibility, yet the same g decomposition treatment exhibits a magnetic gap for the organic spin susceptibility itself. This striking difference between the two classes of compounds is directly correlated to the differences in their structures.

The line-width temperature dependence can be qualitatively related to the above discussion. The line width in $(\text{Et}_4\text{N})_3\text{Nb}_6\text{Cl}_{18}$ varies from 115 G at 300 K to 70 G at 40 K (Figure 10). In $(\text{TMTTF})_2\text{ClO}_4$ the line width varies from 4 G at 300 K to 1.5 G at 80 K.³⁵ In the $(\text{TMTSF})_2\text{X}$ series the line width varies from a few gauss at low temperature to 160–230 G at 300 K depending upon the counteranion.⁴⁵ In 1 and 2 the susceptibility is dominated by the cluster spins at low temperature, and the line width is high (Figure 10). When the temperature is increased, the organic character of the susceptibility increases and the line width decreases. Above 150 K, the observed increase of the line width with temperature is qualitatively comparable to the respective behaviors in the $(\text{TMTTF})_2\text{X}$ and $(\text{TMTSF})_2\text{X}$ series.

Acknowledgment. We warmly thank K. Bechgaard, E. Engler, C. Lenoir, and A. Moradpour for their generous supply of TMTSF and TMTTF during the early stages of this and other related work. We also benefit from the expert experimental assistance as well as stimulating discussions and continuing interest of S. Tomic and D. Jérôme for transport properties and high-pressure experiments and S. S. P. Parkin and J. B. Torrance for magnetic susceptibility studies. We are grateful to J.-Y. Saillard for calculation and discussion of the electronic structure of the niobium clusters. Support from the CNRS (ATP-PIR-MAT Chimie Douce) is gratefully acknowledged.

Registry No. 1, 110670-22-9; 2, 110710-47-9; TMTSF, 55259-49-9; TMTSF⁺, 73261-22-0; TMTTF, 50708-37-7; $(\text{Et}_4\text{N})_3\text{Nb}_6\text{Cl}_{18}$, 12128-45-9; $\text{Nb}_6\text{Cl}_{18}^{4-}$, 12515-95-6; $\text{Nb}_6\text{Cl}_{18}^{3-}$, 12515-94-5; $\text{Nb}_6\text{Cl}_{18}^{2-}$, 12515-93-4; $\text{Nb}_6\text{Cl}_{18}^-$, 124754-11-6; $\text{Bu}_4\text{N}^+\text{PF}_6^-$, 3109-63-5.

Supplementary Material Available: Numbering scheme for the donor molecules, tables of atomic coordinates (including hydrogen and solvent atoms), anisotropic thermal parameters, and all bond lengths and angles for 1 and 2 (26 pages); observed and calculated structure factors for 1 and 2 (26 pages). Ordering information is given on any current masthead page.

(41) Tomkiewicz, Y. *The Physics and Chemistry of Low Dimensional Solids*; Alcácer, L., Ed.; D. Reidel: Dordrecht, The Netherlands, 1980; p 187.

(42) Below 150 K, the organic spins contribution to the total spin susceptibility is very low and on the order of the error bar.

(43) Coulon, C. *J. Phys. (Orsay)* **1983**, *44*, C3-885.

(44) Fukuyama, H.; Rice, T. M.; Varma, C. M.; Halperin, B. I. *Phys. Rev. B* **1974**, *10*, 3775.

(45) Pedersen, H. J.; Scott, J. C.; Bechgaard, K. *Phys. Rev. B* **1981**, *24*, 5014.